JACS
JOURNAL OF THE AMERICAN CHEMICAL SOCIETY
Article
pubs.acs.org/JACS

Noncanonical Stacking Geometries of Nucleobases as a Preferred Target for Solar Radiation

Ruslan R. Ramazanov, Dmitriy A. Maksimov, and Alexei I. Kononov*

Department of Molecular Biophysics and Polymer Physics, St. Petersburg State University, 7/9 Universitetskaya nab., St. Petersburg 199034 Russia

Supporting Information

ABSTRACT: Direct DNA absorption of UVB photons in a spectral range of 290−320 nm of terrestrial solar radiation is responsible for formation of cyclobutane pyrimidine dimers causing skin cancer. Formation of UVB-induced lesions is not random, and conformational features of their hot spots remain poorly understood. We calculated the electronic excitation spectra of thymine, cytosine, and adenine stacked dimers with *ab initio* methods in a wide range of conformations derived from PDB database and molecular dynamics trajectory of thymine-containing oligomer. The stacked dimers with reduced interbase distances in curved, hairpin-like, and highly distorted DNA and RNA structures exhibit excitonic transitions red-shifted up to 0.6 eV compared to the B-form of stacked bases, which makes them the preferred target for terrestrial solar radiation. These results might have important implications for predicting the hot spots of UVB-induced lesions in nucleic acids.

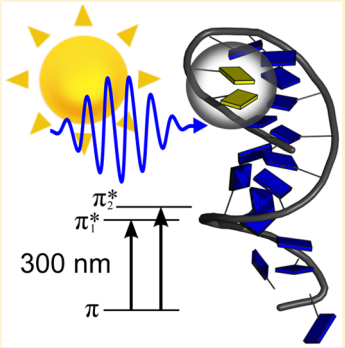

INTRODUCTION

Direct absorption of ultraviolet (UV) radiation by nucleic acids (NAs) can cause various types of damage to both DNA and RNA: dimers formation, photochemical modification, cross-linking, and oxidative damage.[1,2] Cyclobutane pyrimidine dimers (CPDs)[3] are considered as the major UV-induced DNA lesion[4] causing skin cancer.[5,6] UVB spectral range of 290−320 nm was shown to be of primary importance in CPD formation under terrestrial solar radiation. The action spectra of CPD formation in many cases[4,7,8] differ from DNA absorption spectrum, exhibiting a significant intensity in the range about 300 nm where the DNA absorption is very low (Figure 1). This fact means that a minor, highly dimerizable fraction of pyrimidine bases in DNA has a different absorption spectrum, since the quantity of CPDs is the product of the absorbance and the quantum efficiency. The difference between the action spectrum of CPD formation for genomic DNA[4] and the absorption spectrum of thymine containing oligomer[9] (Figure 1) suggests that a fraction of dimerizable pyrimidines has electronic transitions in the 290−300 nm range, ca. 0.5 eV shifted to the red side from the absorption maximum. The product of the action spectrum (or absorption spectrum) and a solar flux spectrum[10] is the effectivity spectrum for formation of the dimers by the terrestrial solar radiation, which reflects the rate of CPD formation (or absorption) at a given wavelength. The effectivity spectra for both major ground state conformation, with the absorption spectrum coinciding with the solution spectrum, and the minor fraction, with absorption spectrum coinciding with the action spectrum, plotted in Figure 1, have a maximum at about 310 nm. The integral effectivity, however, in the case of the minor fraction is much higher compared with that for the major fraction. The minor fraction of stacked pyrimidines with electronic transitions at 300 nm thus appears the most sensitive to solar radiation, and the hot spots of CPD formation under solar radiation might be located in those sites.

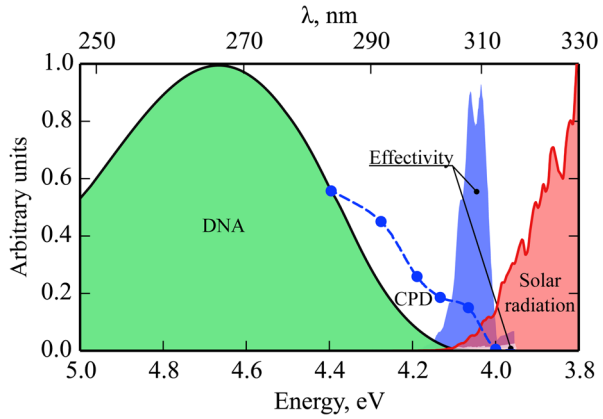

Figure 1. DNA absorption spectrum: $(dT)_{20}$,[9] action spectrum for formation of pyrimidine dimers (plotted from data of immunodot blot assay[4]), UV spectrum of terrestrial solar radiation,[10] and effectivity spectra obtained as the product of the solar spectrum and the absorption or action spectrum.

Properties of Franck−Condon excited states of NAs have been a subject of extensive quantum mechanical (QM) studies with the use of *ab initio* methods and time-dependent density functional theory (TD DFT).[11−20] NA stacked dimers, as a main model system in the high level *ab initio* calculations of

Received: May 18, 2015
Published: August 27, 2015

DOI: 10.1021/jacs.5b05140
J. Am. Chem. Soc. 2015, 137, 11656−11665

vertical transitions, exhibit no markedly red-shifted transitions compared to monomer absorption, apart from a small ∼0.1 eV exciton splitting in homodimers,[11−13] resulting in a weak wavelength tail[11] relative to the monomer's spectrum. Neither increasing the amount of interacting bases in single DNA strand[11,13] nor base pairing[11] in the double strand affect the calculated excitation energy of the lowest-energy excitonic state. The experimental results also show that nearest base−base interactions can indeed satisfactory describe absorption[21] and circular dichroism spectra.[22] It has also been shown that only delocalized excitonic $\pi\pi^*$ states contribute to the low-energy part of the absorption spectra, while charge-transfer (CT) transitions appear to be blue-shifted relative to absorption maximum.[11,12,15−18] Meantime, a significant deviation of the fluorescence excitation spectra of some dinucleotides and oligonucleotides from their absorption spectra in the 290−310 nm region,[21,23,24] a long-wavelength tail in DNA absorption spectra[25,26] suggested possible electronic transitions in that spectral range. The authors of ref 26 stated that even in UVA range above 330 nm CPDs were formed through direct DNA absorption. On the basis of theoretical calculations with the use of TD DFT approach considering also solvent effects, it was proposed that charge transfer states contributed significantly to the long-wavelength tail of DNA absorption due to higher inhomogeneous broadening of CT states.[9,19,20,26] However, in contrast to TD-DFT, QM/MM calculations performed for DNA duplexes at high *ab initio* level show that spectral broadening is mostly caused by intramolecular vibrations,[17] and CT states do not affect the low-energy part of the spectra.[17,18]

All the theoretical studies however dealt with classical A or B stacking geometries,[11−13] artificial,[14,15] optimized or molecular dynamics (MD) sampled geometries[15−20] with interbase distances close to canonical stacking forms. As an exception, it is worth noticing ref 14 where authors studied the geometry dependence of the splitting, and also ref 15 in which the distance dependence of CT states in heterodimers was examined. In living organisms, NAs mostly exist in the canonical forms indeed, but occurrence of some other conformations is also possible, depending on the sequence and local environment conditions.[27] DNA in cell is wound around nucleosomes, being in partially distorted conformation relative to the B form. Moreover, DNA is in single-stranded form during replication process. An unusual stacking geometry in the bent NAs might enhance electron overlap and thus change significantly the electronic spectrum. It has been shown indeed that exciton splitting is very sensitive to interbase distance and rotation angle.[14]

Experimental observation of ultrafast photodimerization of thymine within ∼1 ps[28,29] and QM[30,31] studies clearly show that CPD formation is mainly controlled by conformation of the stacked nucleobases. It has been suggested[32,33] that dimerizable thymine dimers fall into a certain conformational range determined by the distance between the midpoints of the C6−C5 bonds (d) and the dihedral angle C5−C6−C6−C5 (η) marked in Figure 2 for the canonical structure of thymine dimer in B conformation derived from PDB database (ID: 1ENN[34]). Although MD simulations can explain the low quantum yields of CPD formation by the rareness of reactive conformations,[32,33] MD is not able to give reasons for experimentally observed nonrandom distribution of CPDs[35−43] and to predict hot spots of the photolesions in genomic DNA.

In our study, for the first time we addressed the question about the relationship between conformation of the stacked

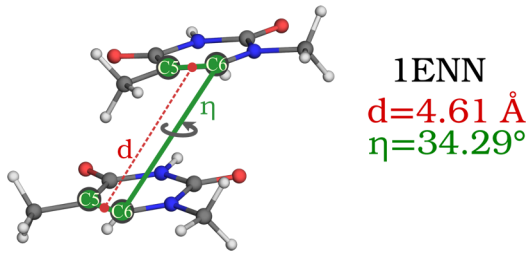

Figure 2. Structure of thymine dimer in canonical B form of DNA from PDB (ID: 1ENN).

bases and their electronic spectra in attempt to explain the observed features in the CPD action spectra and to determine the structures most sensitive to solar radiation. We calculated the spectra of thymine, cytosine, and adenine dimers in a wide range of conformations found in noncanonical NA structures from PDB database and molecular dynamics trajectory of thymine-containing oligomer in comparison with B-form dimers. We based our studies on high level *ab initio* methods that would eliminate uncertainties related to charge transfer states and provide a reliable description for distorted noncanonical structures, and analysis of the nature of the excited states, which may not be accounted for properly in the empirical dispersion correction methods. We found that all the studied dimer conformations within the range of approximately $d \lesssim 3.3$ Å and $\eta \lesssim 50°$ exhibited excitonic transitions red-shifted up to 0.6 eV compared to canonical B-form of stacked bases. Most of these conformations were found in hairpin-like DNA and RNA motifs, and highly distorted B-form DNA structures. We thus conclude that such sites with noncanonical stacked geometries are the preferred spots for CPD formation and other photoproducts under solar radiation.

COMPUTATIONAL METHODS

MD simulations of single-stranded $(dT)_{18}$ oligomer were performed with Gromacs 4.5.5[44] program package with the AMBER parmbsc0 force field.[45] The initial structures of DNA oligomers were constructed in the X3DNA package.[46] The model for the DNA solution utilized periodic boundary conditions for cubic box 14 × 14 × 14 nm and explicit TIP3P water solvent. Negatively charged phosphate groups of DNA were neutralized by the corresponding number of Na^+ counterions. We also added 30 ion pairs of NaCl as ca. 50 mM background electrolyte. The particle mesh Ewald (PME) algorithm[47] was used for calculation of long-range electrostatic interactions. The system was minimized by first restraining the DNA, and then the entire system was allowed to relax. The MD was performed in the NVT ensemble using a Parrinello-Raman thermostat with a 2 fs integration step. The trajectory frames were written every 24 000 integration steps. All H-bonds were constrained using the LINCS algorithm.[48] After 10 ns of the whole system heating up to 350 K and equilibration, 30 ns MD simulations at 310 K were performed to sample the conformational space of the DNA. Analyses of resulting trajectories were performed using MDAnalysis[49] toolkit.

The initial structures of the adenine, cytosine, and thymine homodimers were derived from the PDB structures of DNA/RNA motifs and from the time-frames of MD trajectories. The final geometries of the dimers were constructed by first optimizing the corresponding monomers and then inserting them into an arrangement of the initial PDB dimer geometries. Monomer geometry optimization was performed using resolution of the identity second-order Møller−Plesset perturbation theory (RI-MP2)[50] and aug-cc-pVDZ[51] basis set as implemented in ORCA.[52] In our calculations, we refer to 9-methyladenine as an adenine monomer, 1-methylcytosine as a cytosine monomer, and 1-methylthymine as a thymine monomer. Electronic excitation spectra were calculated using different high level

DOI: 10.1021/jacs.5b05140
J. Am. Chem. Soc. 2015, 137, 11656−11665

computational approaches in vacuum including doubles correction to the excitation energy from configuration interaction with single substitution CIS(D),[53] the approximate coupled cluster model CC2,[54] and the second-order algebraic diagrammatic construction ADC(2)[55] with the resolution of the identity approximation (RI).[56] CIS(D), CC2, and ADC(2) have been proven as reliable and efficient methods for calculating and description of the excited states of DNA fragments,[11−18] including also the conformations with strongly distorted geometries.[12,14−16] ADC(2) method, using a Hermitian secular matrix constructed by many body perturbation theory, was chosen in our study as the major reference method for comparison with the CIS(D) and CC2 results. The calculations for monomers have been performed using the cc-pVDZ, aug-cc-pVDZ, aug-cc-pVTZ,[51] TZVP,[57] and 6-311++G**[58] basis sets. The calculations for the B-form dimers used cc-pVDZ, TZVP, 6-311++G**, and aug-cc-pVDZ basis sets. Since aug-cc-pVDZ and aug-cc-pVTZ showed nearly the same and the most close to experimental maxima results in the case of monomers, we used the aug-cc-pVDZ basis set further when calculating the spectra for the dimers in noncanonical distorted conformations. Since we were interested in the low-energy states of the noncanonical conformations, comprising the red tail of the dimers absorption, 6−8 first states were included at the CC2 and ADC(2) levels for these calculations. For the B-form dimers, we calculated 16 states at the CIS(D) level. Basis set superposition error (BSSE) corrections were not considered since they do not greatly affect the excitation energies.[59] Attachment/detachment density plots were calculated with ORCA program package and viewed utilizing PyMOL.[60] Charts of the structures were prepared by use of Chemcraft[61] and PyMOL. Analysis of the transition density matrix in the atomic orbital basis has been performed with TheoDORE package[62] using the following descriptors:[63−65] PR, the excitonic participation ratio, representing delocalization; CT, the total amount of charge separation (including charge resonance and directed transfer contributions); and CTnet, showing the net charge shifted. CIS(D) calculations were performed in ORCA; CC2 and ADC(2) calculations were performed in TURBOMOLE.[66] All the calculations were performed in the Supercomputing Center of Lomonosov Moscow State University.[67]

RESULTS AND DISCUSSION

Thymine Dimers in MD Simulation. First we obtained the distribution of thermally accessible thymine dimer conformations at different values of d and η for $(dT)_{18}$ oligonucleotide. The obtained distributions are shown in Figure 3 and Figures S1 and S2. Our results are very similar to that obtained earlier[32,68] with somewhat different computation protocols. The number of conformations within the range of $d \lesssim 3.6$ Å (dashed line in Figure 3) is about 5%, which is in agreement with previous estimation. As already proposed,[32,33,68] this fraction of the stacked bases can be referred to as dimerizable dimers since the experimental quantum yield of CPD formation is also a few percent in magnitude.[9] Then, we calculated the electronic spectra of the dimers in a wide conformational range.

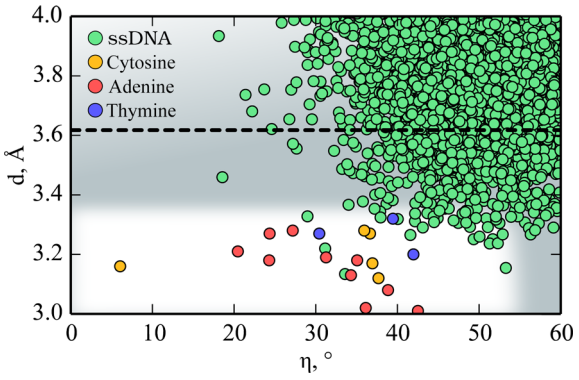

Figure 3. Distributions of thymine dimers at different values of d and η for $(dT)_{18}$ oligonucleotide obtained from MD simulations. Plotted also are the dots indicating d and η for selected thymine, adenine, and cytosine dimers in noncanonical stacking geometries exhibiting the lowest $\pi\pi^*$ states red-shifted by 0.4−0.6 eV from the corresponding B-form maxima.

It appeared that all the thymine dimers obtained from MD trajectories within the conformational range of approximately $d \lesssim 3.3$ Å and $\eta \lesssim 50°$ (highlighted area in the Figure 3), able to produce the *cys*−*syn* isomer[3] of CPD, exhibited electronic transitions red-shifted by ≥0.4 eV from the absorption maximum of canonical B-form dimer. Figure 4 presents

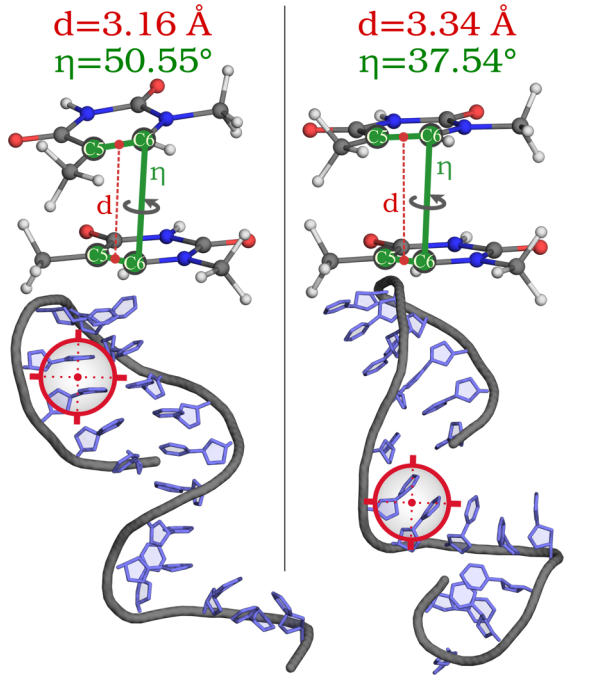

Figure 4. Structures of the thymine dimers from 196th (left) and 518th (right) frames of MD simulation of ssDNA.

examples of two structures containing thymine dimers with reduced interbase distances found in MD trajectory of $(dT)_{18}$. The results of our calculations with CIS(D)/aug-cc-pVDZ approach are summarized in Table S1. CIS(D) calculations with aug-cc-pVDZ basis set (Table S1) somewhat overestimate (by 0.37 eV) the energy of the 4.70 eV absorption maximum of thymine in solution. The agreement with experimental results could be improved by using a more complicated computational approach as shown below and also including environment interactions and considering vibrational effects on the absorption spectrum.[17] As it has been noted above, interaction of adjacent bases and hydrogen bonding in the duplex practically do not affect the position of the lowest-energy $\pi\pi^*$ states (within 0.05 eV).[11,13] QM/MM calculations performed for B-DNA duplexes in solution predict ca. 0.1 eV[18] and 0.4 eV[17] red shifts of the spectra of adenine and adenine−thymine dimers, respectively, relative to vacuum. The exciton splitting, however, remains the same.[18] One can reasonably assume that the environment affects equally the B-form and the distorted dimers. Such approximation, however, should be tested by further QM/MM studies. In our study, we did not include the

DOI: 10.1021/jacs.5b05140
J. Am. Chem. Soc. 2015, 137, 11656−11665

environment in the model since we were interested in the impact of geometry factor on the shift of the lowest exciton state rather than environment effects and absolute values of the energies. Our calculations show that the value of this shift practically does not depend on the computation approach used (Table 1). Although more complicated basis set (Table S2) and computation method tend to shift the transitions to lower energies, thus approaching the position of the maximum to the experimental value, the exciton splitting and the relative shift of the lowest $\pi\pi^*$ state remains the same with accuracy of 0.05 eV (Table 1). In principle, it is not surprising since it has been demonstrated that absolute values of the exciton splitting in the dimers with face-to-face geometry calculated in a wide range of interbase distances and rotation angles are practically independent of the *ab initio* method with accuracy of about 0.05 eV.[14] Here we show that the relative position of the lowest state also does not depend on the computational approach in a wide range of conformations.

Table 1. Vertical Excitations Energies (in eV) for the 4 Lowest Excited Singlet States of Thymine Monomer and Thymine Dimers in the Different Stacking Geometries Obtained with CIS(D) (First Row), ADC(2) (Second Row), and CC2 (Third Row) and the aug-cc-pVDZ Basis Set, Exciton Splitting, and the Shift of the Lowest $\pi\pi^*$ State Relative to the B-Form Dimer

	$n\pi^*$	$n\pi^*$	$\pi\pi^*$	$\pi\pi^*$	ΔE	shift
monomer		4.92		5.07		
		4.53		4.80		
		4.78		4.91		
1ENN	4.83	4.86	4.98	5.08	0.10	
	4.44	4.45	4.68	4.81	0.13	
	4.70	4.71	4.80	4.91	0.11	
518th fr.	4.77	4.80	4.64	5.08	0.44	0.44
from MD	4.35	4.38	4.32	4.80	0.47	0.48
	4.60	4.63	4.44	4.91	0.47	0.47
1BAE	4.74	4.76	4.69	5.08	0.39	0.39
	4.31	4.33	4.42	4.78	0.37	0.39
	4.58	4.62	4.48	4.90	0.42	0.43

Figure 5 illustrates the exciton splitting of the thymine $\pi\pi^*$ and $n\pi^*$ states in the different stacked conformations of the dimer. It is worth noting that the splitting appears to be essentially nonsymmetric, which increases the effect. Since low-intensity $n\pi^*$ states are usually blue-shifted in polar environment with respect to gas phase and do not contribute significantly to the absorption spectra, we do not pay special attention to the $n\pi^*$ states in the dimers.

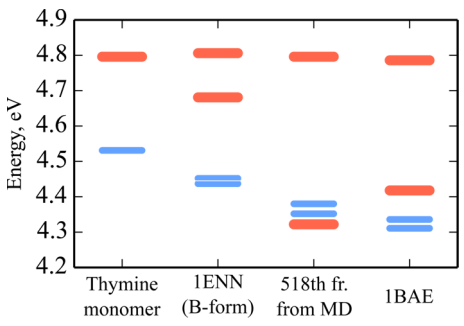

Figure 5. Diagram illustrating the splitting of $n\pi^*$ (blue) and $\pi\pi^*$ (red) excited states in the stacked thymine dimers at different geometries in comparison to the monomer excited state energies. Energies are calculated with the ADC(2)/aug-cc-pVDZ level of theory.

Figures 6, S3, and S4 show the distribution of the shift of the lowest $\pi\pi^*$ state from the B-form maxima for all the studied structures. As can be seen, decreasing both d and η tend to increase the shift of the lowest-energy transition. The geometry dependence of another important spectral parameter, namely oscillator strength, of the lowest $\pi\pi^*$ state is shown in Figure S5. Figure S6 demonstrates that the transition strength appears to decrease on average with decreasing η.

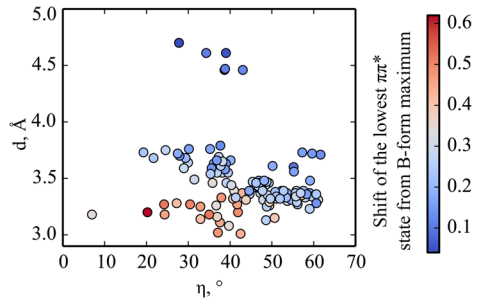

Figure 6. Geometry dependence of the shift of the lowest $\pi\pi^*$ states from the B-form absorption maxima for all the studied dimers.

Thymine Dimers in PDB Structures. The results of MD simulations of $(dT)_{18}$ strand show that relative amount of the thermally achieved thymine structures possessing $\pi\pi^*$ transitions at about 300 nm does not exceed 0.2%. Such low amount of the distorted stacking structures in $(dT)_{18}$ predicted by MD simulations agrees with the fact that the apparent quantum yield of CPD formation in $(dT)_{20}$ was found to be practically constant within 20% experimental error in a wide spectral range up to 310 nm[9]. This means that the action spectrum in that case practically coincides with the DNA absorption spectrum, thus implying a very insignificant amount of the stacking structures absorbing at 300 nm. This is in contrast with the results obtained in some cases for natural genomic DNA, the CPD action spectrum of which differed from the absorption in the 300 nm region, thus indicating more amount of the structures absorbing at 300 nm. The next question we addressed in our study was what structures in natural NAs might favor the distorted dimers with reduced interbase distance. In the $(dT)_{18}$ case, our MD simulations predict that the distorted dimers can be formed at the terminal sites and also in curved and hairpin regions of the thymine chain.

In PDB database we found several examples of noncanonical structures containing neighboring thymines exhibiting red-shifted $\pi\pi^*$ transitions. Thymine dimers with $d \lesssim 3.3$ Å and $\eta \lesssim 50°$ (blue dots in Figure 2) found in i-motif 1BAE[69] (Figure 7), dsDNAs containing thymine−thymine mismatch (2LL9,[70] Figure S7) and abasic site (1FZS,[71] Figure S8) revealed low-lying $\pi\pi^*$ states red-shifted by 0.4−0.5 eV from the B-form maximum (Tables 1 and S1).

Effectivity Spectra of the Dimers. To compare the integral absorption rates of the bases stacked in different geometries in the range of the spectrum of terrestrial solar radiation, vibronic structure of the spectra (causing the major broadening[17]) was modeled by convolution of the spectra obtained with ADC/aug-cc-pVDZ approach with experimental

DOI: 10.1021/jacs.5b05140
J. Am. Chem. Soc. 2015, 137, 11656−11665

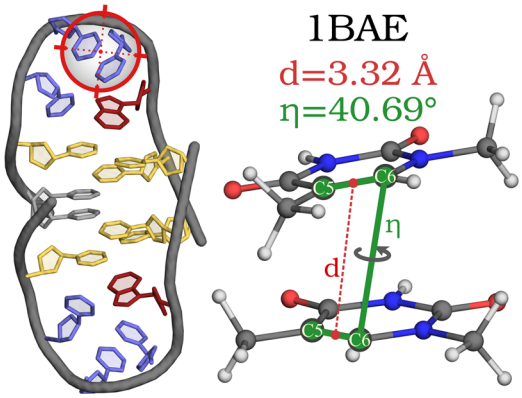

Figure 7. Structure of thymine dimer in i-Motif (PDB ID: 1BAE).

absorption spectrum of thymine fitted by extreme curve (Figure S9).

Typical spectrum of the distorted thymine dimer (1BAE) in comparison with the B-form dimer is shown in Figure 8.

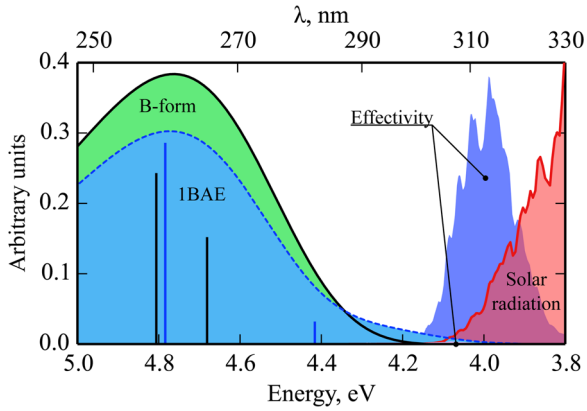

Figure 8. Absorption spectra of the thymine dimers in B-form (PDB ID: 1ENN) and noncanonical stacking (PDB ID: 1BAE) geometries obtained at the ADC(2)/aug-cc-pVDZ level and convoluted with the monomer absorption spectrum to account for vibronic structure of the transitions (vertical sticks indicate positions of $\pi\pi^*$ states), effectivity spectra obtained as the products of the absorption spectra and the spectrum of solar radiation.

Qualitatively, the difference between absorption spectra of B-form and the distorted dimer is similar to the difference observed between the CPD action spectrum and poly(dT) absorption spectrum shown in Figure 1. A long-wavelength tail is clearly seen in the absorption spectrum of the distorted dimer in comparison with the canonical dimer. Progressively growing intensity of solar radiation in this spectral range provides a significant increase in the relative amount of the photons absorbed by the distorted thymine dimers and, hence, their relatively high sensitivity to the radiation. Quantitatively, it can be clearly seen from comparison of the effectivity spectra obtained for the B-form and distorted dimers by multiplication of the corresponding absorption spectra and the spectrum of solar radiation (Figure 8). Integral effectivity, i.e., the absorption rate, in the case of the distorted dimer is ca. 2 orders of magnitude higher than that for the B-form dimer. However, one should be careful with such quantitative estimation of the effect. Although the simplest assumption is that the line-shape may be described by monomeric function seems reasonable, since it accounts for both vibronic structure and inhomogeneities using the experimental curve, the shape might be changed for the dimer. While inhomogeneous broadening has a minor effect on the line-shape,[17] vibronic structure of the band might be altered in the dimer with reduced interbase distance and this should be further examined at high *ab initio* level. Of course, more correct description of vibronic transitions and environmental effects might alter the ratio of the effectivities. However, one can believe that, qualitatively, the difference between B-form dimer and a dimer with reduced interbase distance will remain the same. It should also be noted, that sensitivity of oscillator strength of the lowest transition to the dimer conformation, especially to η as can be seen from Figure S6, also affects significantly the magnitude of the integral effectivity. For example, decreasing η in the structure of 518th frame dimer in comparison with 1BAE increases the red shift (Table S1), but decreasing η also lowers oscillator strength of the transition (Table S1, Figure S6).

Absorption rate that dramatically increases in the distorted dimers is not the only factor affecting the sensitivity of NA structures to solar radiation. Rate of photochemical reaction is a product of both absorption rate and quantum yield. Both experimental[28,29] and theoretical[20,30,31] studies suggest that the efficiency (quantum yield) of CPD formation is strongly conformationally dependent, while solvent has no effect on the photoreactivity.[20] The photodimerization proceeds via a singlet excited state at a configuration near the conical intersection (S0/S1−CI) geometry. Insignificant yield of CPD formation in DNA from triplet state is probably also possible, since it takes place in thymine solution.[72] The triplet mechanism likely becomes important in UVA range where sensitized photoreactions via triplet−triplet energy transfer[73] are probably dominant. The conformational range for thymine dimerization is not quite understood. Theoretical QM studies predict that the CI can be reached at $d < 3.6–4$ Å,[20,68] which is close to the empirical estimations of MD simulation.[32,33,68] MD simulations also predict the cutoff for dihedral angle to be 30−50°. However, QM calculations indicate that the dimer formation can proceed at substantially higher values.[20,68] Since the observed dimer conformations with significantly red-shifted transitions evidently appear to be within the predicted range for the dimerizable dimers, it seems reasonable to assume that the quantum yield in the dimers with unusual stacking geometry with $d \lesssim 3.3$ Å and $\eta \lesssim 50°$ could be at least not less than that for the major fraction of dimerizable dimers having the absorption spectrum close to the B-form spectrum. In this case, the obtained above effectivity spectra reflect indeed much higher sensitivity to solar radiation for the distorted stacking dimers found in some noncanonical DNA structures.

Adenine and Cytosine Dimers in PDB Structures. Thymine is not the only potential target for solar radiation. Cytosine, although to less extent, can also undergo dimerization.[1] The less photoreactivity for cytosine compared with thymine was explained by the existence of stable excimer-like states below (S1/S0) CI.[74] Though CPDs and also pyrimidine (6–4) pyrimidone adducts[1] (with a 10-fold lower yield) are the most frequent lesions in DNA, direct absorption of terrestrial solar radiation in UVB range can also lead to other photoproducts and photochemical reactions in DNA and RNA. For example, adenine can undergo dimerization.[75] UV-induced formation of 8-hydroxy-deoxyguanosine in DNA (but not in guanine) was also observed.[76] It has recently been shown that stacking and base pairing can lead to photoinduced electron and proton transfer.[77,78] Possible photochemical events in DNA

DOI: 10.1021/jacs.5b05140
J. Am. Chem. Soc. 2015, 137, 11656−11665

are thus not limited to pyrimidine bases. In this respect, it is interesting to examine the spectra of other nucleobase dimers. We studied below cytosine and adenine dimers, also able to form photoproducts upon direct UV absorption, in both DNA and RNA structures.

The observed red-shifted transitions in the distorted base-stacking conformations are not a unique feature of thymine staked bases in DNA. We also show that other bases in noncanonical DNA/RNA structures can exhibit similar effect as well. Red and yellow dots in Figure 2 indicate adenine and cytosine dimers, respectively, in DNA/RNA structures derived from PDB database, possessing the geometry that falls within the range of d and η determined above. Figure 9 (at left) and

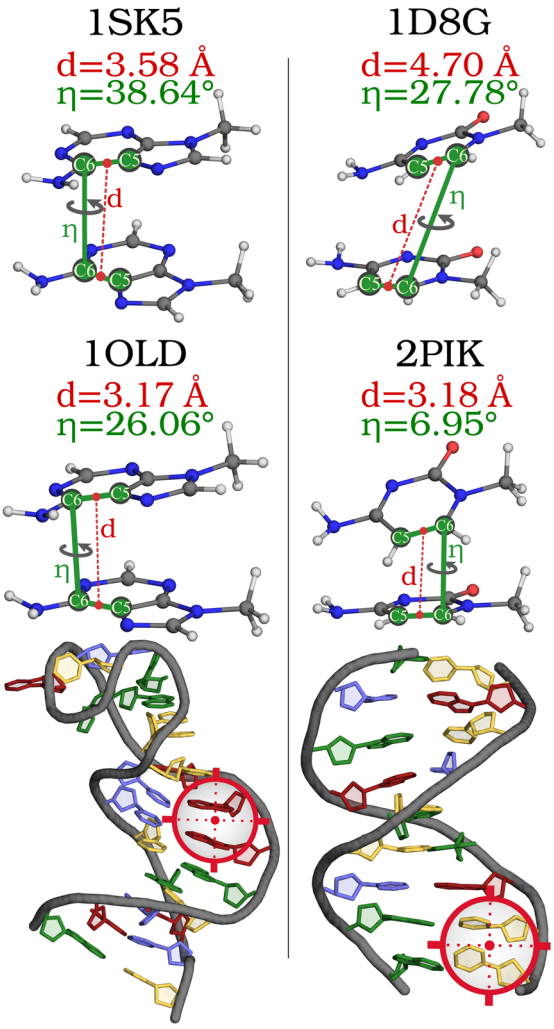

Figure 9. Structures of adenine (left) and cytosine (right) dimers in canonical B forms (upper row) and noncanonical structures (bottom) from PDB database.

Figure S10 show hairpin DNA aptamer 1OLD[79] and highly distorted B-form DNA 1ZF0[80] structures containing adenine dimers with unusual stacking geometry in comparison with the B-form dimer (PDB ID: 1SK5). Figure 9 (at right) and Figure S11 show ligand−DNA complex 2PIK[81] and stem-loop RNA 1T28[82] containing distorted cytosine dimers in comparison with the B-form dimer (1D8G[83]). The excited states calculated for the dimers are presented in Tables 2 and 3 in comparison with the corresponding B-form dimers. Like in the case of thymine dimers, the spectra exhibit low-lying excitonic transitions significantly red-shifted by ca. 0.5 eV from the corresponding B-form maxima. Energies of $\pi\pi^*$ states and geometric parameters of all the studied thymine, adenine and cytosine structures are summarized in Table S1.

Nature of Low-Energy States. As already noted above, CT states do not affect the long-wavelength part of DNA absorption spectrum.[11,12,15−18] Nevertheless, we addressed the question of whether CT interactions contribute to the low-energy states in the dimers with reduced interbase distances. To investigate the nature of the red-shifted transitions, we calculated the distributions of the attachment/detachment electron density and performed the analysis of structure of the low-lying excited states in the studied structures using the descriptors suggested in ref 65. As can be seen from the attachment/detachment density maps (Chart 1), the lowest-energy $\pi\pi^*$ states in all the distorted dimers are delocalized over two bases like in the case of the B-form dimers, and the transitions are mostly of $\pi\pi^*$ excitonic character. The values of participation ratio (PR), i.e., the number of coherently coupled chromophores, close to 2 support that conclusion (Table 4). A slight overlapping of the densities in the case of the distorted dimers indicates a possible contribution of charge or charge-resonance terms. The detailed description of the structure of the excited states shows indeed that charge-transfer interactions slightly contribute to the lowest $\pi\pi^*$ states (Table 4). This can be seen from an increase in the CT values up to about 0.1−0.2 for the thymine and cytosine structures and up to 0.4 for adenine 1OLD dimer. However, for the thymine and cytosine dimers, net charge shift (CTnt) remains negligible, which is indicative of charge-resonance rather than charge transfer term. For adenine 1OLD dimer, the values of CT and CTnt indicate that both charge-resonance and charge-transfer terms partly contribute to the lowest $\pi\pi^*$ state. The above analysis shows that the significant red shift of the low-energy transitions in the distorted base-stacking conformations with respect to B-form DNA is obviously caused by the enhanced excitonic coupling due to reducing interbase distance in the case of noncanonical stacking. The slight contribution of the CT and charge-resonance interactions can alter the environment effects in the case of the distorted dimers. The state character can also be affected by interactions with neighboring bases.[17] These probable effects should be further examined, since they may affect the spectra of noncanonical conformations of the dimers.

Noncanonical Stacking Geometries and Hot Spots of UV-Induced NA Lesions. Many experimental studies reveled that UV-induced DNA lesions were distributed not randomly in DNA. It has been shown that formation of the photoproducts is strongly sequence and conformation dependent.[35−43] Most studies on the conformation and sequence effects dealt with UVC irradiation. However, the results on UVC-induced lesions in some cases differ from that upon UVB and SSL irradiation.[38−40] Our data provide one more insight on the origin of the observed effects and potential hot spots of photoproduct formation in NAs. As it follows from our calculations, the stacked bases with reduced interbase distances within the conformational range of $d \lesssim 3.3$ Å and $\eta \lesssim 50°$ appear to be much more sensitive to the terrestrial solar radiation due to significant value of exciton splitting and consequently low-lying $\pi\pi^*$states in those structures in comparison with B-form stacked bases. Such stacking geometries are obviously the preferred targets for terrestrial solar radiation. In UVC range, where spectral difference between

DOI: 10.1021/jacs.5b05140
J. Am. Chem. Soc. 2015, 137, 11656−11665

Table 2. Vertical Excitations Energies (in eV) for the 6 Lowest Excited Singlet States of Adenine Monomer and Adenine Dimers in the Different Stacking Geometries Obtained with CIS(D) (First Row), ADC(2) (Second Row), and CC2 (Third Row) and the aug-cc-pVDZ Basis Set, Exciton Splitting, and the Shift of the Lowest $\pi\pi^*$ State Relative to the B-Form Dimer

	nπ*	nπ*	ππ*	ππ*	ππ*	ππ*	ΔE	shift
monomer		5.52			5.28	5.29		
		4.96			5.01	5.07		
		5.05			5.11	5.11		
1SK5	5.42	5.43	5.13	5.26	5.27	5.29	0.16	
	4.89	4.92	4.83	4.96	5.02	5.05	0.21	
	4.98	5.01	4.92	5.06	5.07	5.09	0.18	
1OLD	5.15	5.22	4.82	5.22	5.25	5.28	0.46	0.47
	4.75	4.81	4.50	4.90	4.93	5.04	0.54	0.55
	4.83	4.89	4.57	4.92	5.09	5.11	0.54	0.53

Table 3. Vertical Excitations Energies (in eV) for the 4 Lowest Excited Singlet States of Cytosine Monomer and Cytosine Dimers in the Different Stacking Geometries Obtained with CIS(D) (First Row), ADC(2) (Second Row), and CC2 (Third Row) and the aug-cc-pVDZ Basis Set, Exciton Splitting, and the Shift of the Lowest $\pi\pi^*$ State Relative to the B-Form Dimer

	nπ*	nπ*	ππ*	ππ*	ΔE	shift
monomer		5.10		4.59		
		4.63		4.35		
		4.83		4.53		
1D8G	5.00	5.01	4.52	4.56	0.04	
	4.45	4.51	4.26	4.30	0.04	
	4.68	4.72	4.45	4.49	0.04	
2PIK	4.75	4.96	4.22	4.65	0.43	0.34
	4.38	4.44	3.97	4.29	0.32	0.33
	4.60	4.66	4.14	4.49	0.35	0.35

Chart 1. Attachement/Detachement Electron Densities for the Lowest $\pi\pi^*$ States of Thymine, Adenine, and Cytosine Dimers at Different Geometries

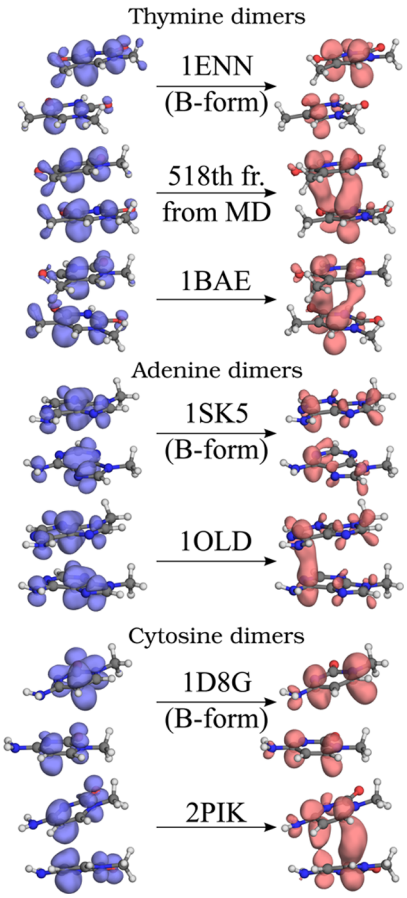

stacking conformations is not essential, the photochemical selectivity of the distorted stacked dimers might be caused by their low-lying excited states serving as a trap for excitation energy transfer from neighboring bases. The effect of just energy trapping might be important in the UVB range as well, especially in the case when oscillator strength of the lowest state appears to be low enough. Efficient energy migration, seen in some experiments with dyes[84,85] or in polarization studies on femtosecond time scale,[86,87] to the lowest-energy states of such dimers could in principle make them as the most probable reaction centers of subsequent photochemistry.

Rare base-stacking forms with significant absorption in 290−300 nm region due to large exciton splitting were observed in our earliest experimental studies.[21,23,24] As in the case of the most dimerizable thymine dimers absorbing in the long-wavelength spectral range, seen in the action spectrum in Figure 1, minor forms of stacked bases with significant absorption above 290 nm were seen in the fluorescence excitation spectra of polymeric forms of NAs due to their relatively high quantum yield compared to the major fraction of the bases. The comparison of the efficiency spectra for canonical and distorted dimers (Figure 8) predict that such distorted stacking conformations would become biologically significant at concentrations above ∼1% relative to the total amount of the bases that can undergo a given photochemical damage with the same quantum efficiency. For example, in the case of thymine oligonucleotide, the concentration of all dimerizable thymines is about 5%. The estimated above amount of the conformations with the red-shifted transitions is ca. 0.2%. Such amount is enough so that at 100-fold higher absorption, 80% of CPDs are formed by thymines being in the distorted conformations.

Concentration of the stacked bases with such distorted stacking geometry in NAs is evidently determined by their secondary structure. Revealing the structures in which such distorted stacked dimers may be realized is of great importance for determining the hot spots of CPD and other photoproduct formation. Our observations show that the dimers with reduced interbase distances are most frequently observed in the curved and hairpin-like NA structures. This is in line with some experimental findings that photoproduct formation is increased at the site of the kink in DNA.[36] Unwinding DNA during

DOI: 10.1021/jacs.5b05140
J. Am. Chem. Soc. 2015, 137, 11656−11665

Table 4. Excitation Energies (E, eV), Oscillator Strengths (f), Statistical Descriptors, and Type Assignments at the ADC(2)/aug-cc-pVDZ Level for the Low-Energy Excited States of Thymine, Adenine, and Cytosine Dimers at Different Geometries

assignment	E (eV)	f	PR	CT	CTnt
		TT B-Form 1ENN			
$n\pi^*$	4.44	0.000	0.99	−0.02	0.04
$n\pi^*$	4.45	0.000	0.97	−0.04	−0.05
$\pi\pi^*$	4.68	0.152	1.03	−0.03	−0.06
$\pi\pi^*$	4.81	0.243	0.98	−0.08	0.12
		TT 1BAE			
$n\pi^*$	4.31	0.004	1.21	0.09	0.02
$n\pi^*$	4.33	0.005	1.34	0.20	0.02
$\pi\pi^*$	4.42	0.032	1.98	0.15	−0.01
$\pi\pi^*$	4.78	0.286	1.98	−0.03	0.02
		TT 518th Frame from MD			
$n\pi^*$	4.35	0.005	1.97	0.06	−0.02
$n\pi^*$	4.38	0.006	1.63	0.02	0.10
$\pi\pi^*$	4.32	0.012	1.79	0.11	−0.02
$\pi\pi^*$	4.80	0.310	1.98	−0.04	0.03
		AA B-Form 1SK5			
$n\pi^*$	4.89	0.019	1.53	0.05	0.03
$n\pi^*$	4.92	0.023	1.90	0.13	0.01
$\pi\pi^*$	4.83	0.038	1.92	0.09	0.04
$\pi\pi^*$	4.96	0.220	1.98	0.12	−0.04
$\pi\pi^*$	5.02	0.012	1.82	0.18	0.10
$\pi\pi^*$	5.05	0.114	1.67	0.29	0.00
		AA 1OLD			
$n\pi^*$	4.75	0.018	1.90	0.36	−0.17
$n\pi^*$	4.81	0.008	1.23	0.20	0.05
$\pi\pi^*$	4.50	0.021	1.95	0.42	−0.16
$\pi\pi^*$	4.90	0.154	1.87	0.40	−0.24
$\pi\pi^*$	4.93	0.024	1.94	0.42	−0.17
$\pi\pi^*$	5.04	0.169	1.97	0.13	0.13
		CC B-Form 1D8G			
$n\pi^*$	4.45	0.001	1.06	0.05	0.05
$n\pi^*$	4.51	0.001	1.10	0.08	−0.06
$\pi\pi^*$	4.26	0.035	1.25	0.00	0.00
$\pi\pi^*$	4.30	0.087	1.24	0.01	0.02
		CC 2PIK			
$n\pi^*$	4.38	0.001	1.03	0.03	0.02
$n\pi^*$	4.44	0.001	0.98	−0.02	0.03
$\pi\pi^*$	3.97	0.001	1.98	0.18	−0.09
$\pi\pi^*$	4.29	0.106	1.96	−0.05	−0.01

replication provides a certain flexibility of the bases allowing them to form stacking structures with reduced interbase distances. However, significant local conformational deviations may also occur even in double-stranded B form of DNA, which result from so-called sequence effects, as it takes place in the case of 1ZF0 structure[80] that exhibits an adenine dimer with significantly red-shifted $\pi\pi^*$ state. In other structures studied in this work, where the interbase distance appeared to be less than 3.3 A, the native B form was violated by the interaction with ligands (2PIK) or mismatches (2LL9, 1FZS). In this respect, it can be noticed that experimental results showed that hot spots for UV-induced pyrimidine dimer formation in vivo were concentrated in transcription factor binding sites[37] where native B form might be distorted by interaction with proteins. It should be also noted that some of the dimers with red-shifted $\pi\pi^*$ states were observed at terminal sites of the strands. In the case of cellular DNA, terminal sites can be formed due to strand breaks, which may occur through various DNA-damage and other processes in living cells.

Significant difference in the spectra of the distorted structures from canonical forms of stacking suggests a wavelength dependence of the photoproducts formation. Indeed, it was shown earlier that the sequence-specific distribution of DNA photoproducts was wavelength dependent.[38−40] In some cases it was explained by red shift of methyl-cytosine absorption spectrum compared to thymine.[40,41] The red-shifted transitions in the distorted stacked structures observed in our study can be one more factor contributing to the difference between the mutational spectra of UVB and UVC radiation. All those distorted stacking structures, as it follows from their electronic spectra, are the most sensitive to terrestrial solar radiation. Detailed structural analysis and calculations of the spectra along with photochemical studies might be further helpful in revealing the potential hot spots in NAs. It is also worth noting that the distribution of the photoproducts in NAs caused by native terrestrial solar radiation with significant intensity at 300 nm might be quite different from the distributions that used to be obtained with UVC radiation at 254 nm for the reasons stated above.

CONCLUSION

In conclusion, our results highlight some principle aspects. The most important is that the distorted base-stacking conformations found in curved, hairpin-like, and highly distorted B-form NA structures exhibit significantly red-shifted electronic transitions of excitonic nature, which evidently increases the effectivity of absorption of terrestrial solar radiation, the intensity of which becomes significant in the region about 300 nm where the absorption of canonical forms of NAs falls dramatically. The low-lying excited states in such structures may also serve as a trap for efficient energy transfer from neighboring bases, thus favoring subsequent photochemical events at the certain site. The observed effects are not restricted to only pyrimidine bases, exposed to formation of CPDs as the most dangerous lesions in DNA. They can be relevant as well to other DNA/RNA sun-induced photochemistry. One can thus conclude that such sites with noncanonical stacked geometries with low-lying excited states are the preferred targets for terrestrial solar radiation. Low-lying excited states, as the found spectroscopic signature, might also be an advantage in revealing such noncanonical motifs in natural NAs.

ASSOCIATED CONTENT

Supporting Information

The Supporting Information is available free of charge on the ACS Publications website at DOI: 10.1021/jacs.5b05140.

Distributions of conformational and spectral parameters, illustrations, and geometries of the studied structures (PDF)

AUTHOR INFORMATION

Corresponding Author

*alexei.kononov@pobox.spbu.ru, a.kononov@spbu.ru.

Notes

The authors declare no competing financial interest.

DOI: 10.1021/jacs.5b05140
J. Am. Chem. Soc. 2015, 137, 11656−11665

■ ACKNOWLEDGMENTS

The authors acknowledge Saint-Petersburg State University for a research Grant 11.38.221.2014. The reported calculations were performed in the Supercomputing Center of Lomonosov Moscow State University.[67]

■ REFERENCES

(1) Cadet, J.; Mouret, S.; Ravanat, J.-L.; Douki, T. *Photochem. Photobiol.* **2012**, *88*, 1048−1065.
(2) Wurtmann, E. J.; Wolin, S. L. *Crit. Rev. Biochem. Mol. Biol.* **2009**, *44*, 34−49.
(3) Fisher, G. J.; Johns, H. E.; Wang, S. Y., Eds; *Photochemistry and Photobiology of Nucleic Acids*; Academic Press: New York, 1976; Vol. *1*, pp 225−294.10.1016/B978-0-12-734601-4.50011-2
(4) Besaratinia, A.; Yoon, J.-I.; Schroeder, C.; Bradforth, S. E.; Cockburn, M.; Pfeifer, G. P. *FASEB J.* **2011**, *25*, 3079−3091.
(5) Brash, D. E.; Rudolph, J. A.; Simon, J. A.; Lin, A.; McKenna, G. J.; Baden, H. P.; Halperin, A. J.; Pontén, J. *Proc. Natl. Acad. Sci. U. S. A.* **1991**, *88*, 10124−10128.
(6) You, Y. H.; Szabó, P. E.; Pfeifer, G. P. *Carcinogenesis* **2000**, *21*, 2113−2117.
(7) Freeman, S. E.; Hacham, H.; Gange, R. W.; Maytum, D. J.; Sutherland, J. C.; Sutherland, B. M. *Proc. Natl. Acad. Sci. U. S. A.* **1989**, *86*, 5605−5609.
(8) Garcés, F.; Dávila, C. A. *Photochem. Photobiol.* **1982**, *35*, 9−16.
(9) Banyasz, A.; Douki, T.; Improta, R.; Gustavsson, T.; Onidas, D.; Vayá, I.; Perron, M.; Markovitsi, D. *J. Am. Chem. Soc.* **2012**, *134*, 14834−14845.
(10) ASTM G173-073 standard tables of reference solar spectral irradiances: Terrestrial Global 37 deg South Facing Tilt: http://rredc.nrel.gov/solar/spectra/am1.5/ASTMG173/ASTMG173.html.
(11) Lange, A. W.; Herbert, J. M. *J. Am. Chem. Soc.* **2009**, *131*, 3913−3922.
(12) Spata, V. A.; Matsika, S. *J. Phys. Chem. A* **2013**, *117*, 8718−8728.
(13) Ritze, H.-H.; Hobza, P.; Nachtigallová, D. *Phys. Chem. Chem. Phys.* **2007**, *9*, 1672−1675.
(14) Kozak, C. R.; Kistler, K. A.; Lu, Z.; Matsika, S. *J. Phys. Chem. B* **2010**, *114*, 1674−1683.
(15) Aquino, A. J. A.; Nachtigallova, D.; Hobza, P.; Truhlar, D. G.; Hättig, C.; Lischka, H. *J. Comput. Chem.* **2011**, *32*, 1217−1227.
(16) Plasser, F.; Lischka, H. *Photochem. Photobiol. Sci.* **2013**, *12*, 1440−1452.
(17) Plasser, F.; Aquino, A. J. A.; Hase, W. L.; Lischka, H. *J. Phys. Chem. A* **2012**, *116*, 11151−11160.
(18) Spata, V. A.; Matsika, S. *J. Phys. Chem. A* **2014**, *118*, 12021−12030.
(19) Improta, R.; Barone, V. *Angew. Chem.* **2011**, *123*, 12222−12225.
(20) Improta, R. *J. Phys. Chem. B* **2012**, *116*, 14261−14274.
(21) Kononov, A. I.; Bakulev, V. M.; Rapoport, V. L. *J. Photochem. Photobiol., B* **1993**, *19*, 139−144.
(22) Kadhane, U.; Holm, A. I. S.; Hoffmann, S. V.; Nielsen, S. B. *Phys. Rev. E* **2008**, *77*, 21901−21904.
(23) Rapoport, V. L.; Kononov, A. I. *Dokl. Akad. Nauk SSSR* **1988**, *298*, 231−235.
(24) Kononov, A. I.; Bukina, M. N. *J. Biomol. Struct. Dyn.* **2002**, *20*, 465−471.
(25) Sutherland, J. C. C.; Griffin, K. P. P. *Radiat. Res.* **1981**, *86*, 399−410.
(26) Banyasz, A.; Vayá, I.; Changenet-Barret, P.; Gustavsson, T.; Douki, T.; Markovitsi, D. *J. Am. Chem. Soc.* **2011**, *133*, 5163−5165.
(27) Potaman, V. N.; Sinden, R. R. In *Madame Curie Bioscience Database [Internet]*; Landes Bioscience: Austin, TX, 2000-.
(28) Schreier, W. J.; Schrader, T. E.; Koller, F. O.; Gilch, P.; Crespo-Hernández, C. E.; Swaminathan, V. N.; Carell, T.; Zinth, W.; Kohler, B. *Science* **2007**, *315*, 625−629.
(29) Schreier, W. J.; Kubon, J.; Regner, N.; Haiser, K.; Schrader, T. E.; Zinth, W.; Clivio, P.; Gilch, P. *J. Am. Chem. Soc.* **2009**, *131*, 5038−5039.
(30) Boggio-Pasqua, M.; Groenhof, G.; Schäfer, L. V.; Grubmüller, H.; Robb, M. A. *J. Am. Chem. Soc.* **2007**, *129*, 10996−10997.
(31) Blancafort, L.; Migani, A. *J. Am. Chem. Soc.* **2007**, *129*, 14540−14541.
(32) Johnson, A. T.; Wiest, O. *J. Phys. Chem. B* **2007**, *111*, 14398−14404.
(33) Law, Y. K.; Azadi, J.; Crespo-Hernández, C. E.; Olmon, E.; Kohler, B. *Biophys. J.* **2008**, *94*, 3590−3600.
(34) Soler-López, M.; Malinina, L.; Subirana, J. A. *J. Biol. Chem.* **2000**, *275*, 23034−23044.
(35) Brash, D. E.; Haseltine, W. A. *Nature* **1982**, *298*, 189−192.
(36) Becker, M. M.; Lesser, D.; Kurpiewski, M.; Baranger, A.; Jen-Jacobson, L. *Proc. Natl. Acad. Sci. U. S. A.* **1988**, *85*, 6247−6251.
(37) Pfeifer, G. P.; Drouin, R.; Riggs, A. D.; Holmquist, G. P. *Mol. Cell. Biol.* **1992**, *12*, 1798−1804.
(38) Tyrrell, R. M. *Mutat. Res., Fundam. Mol. Mech. Mutagen.* **1984**, *129*, 103−110.
(39) Mitchell, D. L.; Jen, J.; Cleaver, J. E. *Nucleic Acids Res.* **1992**, *20*, 225−229.
(40) Pfeifer, G. P.; Besaratinia, A. *Photochem. Photobiol. Sci.* **2012**, *11*, 90−97.
(41) Tommasi, S.; Denissenko, M. F.; Pfeifer, G. P. *Cancer Res.* **1997**, *57*, 4727−4730.
(42) Gale, J. M.; Nissen, K. A.; Smerdon, M. J. *Proc. Natl. Acad. Sci. U. S. A.* **1987**, *84*, 6644−6648.
(43) Selleck, S. B.; Majors, J. *Nature* **1987**, *325*, 173−177.
(44) Pronk, S.; Páll, S.; Schulz, R.; Larsson, P.; Bjelkmar, P.; Apostolov, R.; Shirts, M. R.; Smith, J. C.; Kasson, P. M.; van der Spoel, D.; Hess, B.; Lindahl, E. *Bioinformatics* **2013**, *29*, 845−854.
(45) Pérez, A.; Marchán, I.; Svozil, D.; Sponer, J.; Cheatham, T. E.; Laughton, C. A.; Orozco, M.; Pe, A.; Cheatham, T. E., III *Biophys. J.* **2007**, *92*, 3817−3829.
(46) Lu, X.-J. *Nucleic Acids Res.* **2003**, *31*, 5108−5121.
(47) Darden, T.; York, D.; Pedersen, L. *J. Chem. Phys.* **1993**, *98*, 10089−10092.
(48) Hess, B.; Bekker, H.; Berendsen, H. J. C.; Fraaije, J. G. E. M. *J. Comput. Chem.* **1997**, *18*, 1463−1472.
(49) Michaud-Agrawal, N.; Denning, E. J.; Woolf, T. B.; Beckstein, O. *J. Comput. Chem.* **2011**, *32*, 2319−2327.
(50) Bernholdt, D. E.; Harrison, R. J. *Chem. Phys. Lett.* **1996**, *250*, 477−484.
(51) Dunning, T. H. *J. Chem. Phys.* **1989**, *90*, 1007−1023.
(52) Neese, F. *Wiley Interdiscip. Rev. Comput. Mol. Sci.* **2012**, *2*, 73−78.
(53) Head-Gordon, M.; Rico, R. R. J.; Oumi, M.; Lee, T. J. T. *Chem. Phys. Lett.* **1994**, *219*, 21−29.
(54) Christiansen, O.; Koch, H.; Jørgensen, P. *Chem. Phys. Lett.* **1995**, *243*, 409−418.
(55) Trofimov, A. B.; Schirmer, J. *J. Phys. B: At., Mol. Opt. Phys.* **1995**, *28*, 2299−2324.
(56) Hättig, C.; Weigend, F. *J. Chem. Phys.* **2000**, *113*, 5154−5161.
(57) Schäfer, A.; Huber, C.; Ahlrichs, R. J. *J. Chem. Phys.* **1994**, *100*, 5829−5835.
(58) Hariharan, P. C.; Pople, J. A. *Mol. Phys.* **1974**, *27*, 209−214.
(59) Santoro, F.; Barone, V.; Improta, R. *J. Comput. Chem.* **2008**, *29*, 957−964.
(60) The PyMOL Molecular Graphics System, Version 1.5.0.4, Schrödinger, LLC..
(61) Chemcraft. http://www.chemcraftprog.com.
(62) TheoDore. http://theodore-qc.sourceforge.net/index.html.
(63) Tretiak, S.; Mukamel, S. *Chem. Rev.* **2002**, *102*, 3171−3212.
(64) Luzanov, A. V.; Zhikol, O. A. *Int. J. Quantum Chem.* **2010**, *210*, 902−924.
(65) Plasser, F.; Lischka, H. *J. Chem. Theory Comput.* **2012**, *8*, 2777−2789.
(66) Ahlrichs, R.; Bär, M.; Häser, M.; Horn, H.; Kölmel, C. *Chem. Phys. Lett.* **1989**, *162*, 165−169.

DOI: 10.1021/jacs.5b05140
J. Am. Chem. Soc. 2015, 137, 11656−11665

(67) Voevodin, Vl. V.; Zhumatiy, S. A.; Sobolev, S. I.; Antonov, A. S.; Bryzgalov, P. A.; Nikitenko, D. A.; Stefanov, K. S.; Voevodin, Vad. V. *Open Syst. J.: Moscow Open Syst. Publ.* **2012**, *7*, 36−39.
(68) McCullagh, M.; Hariharan, M.; Lewis, F. D.; Markovitsi, D.; Douki, T.; Schatz, G. C. *J. Phys. Chem. B* **2010**, *114*, 5215−5221.
(69) Nonin, S.; Phan, A. T.; Leroy, J. L. *Structure* **1997**, *5*, 1231−1246.
(70) Jourdan, M.; Granzhan, A.; Guillot, R.; Dumy, P.; Teulade-Fichou, M.-P. *Nucleic Acids Res.* **2012**, *40*, 5115−5128.
(71) Smirnov, S.; Matray, T. J.; Kool, E. T.; de los Santos, C. *Nucleic Acids Res.* **2002**, *30*, 5561−5569.
(72) Whillans, D. W.; Johns, H. E.; Whillans, D. W. *J. Am. Chem. Soc.* **1971**, *93*, 1358−1362.
(73) Cuquerella, M. C.; Lhiaubet-Vallet, V.; Bosca, F.; Miranda, M. A. *Chem. Sci.* **2011**, *2*, 1219−1232.
(74) Serrano-Pérez, J. J.; González-Ramírez, I.; Coto, P. B.; Merchán, M.; Serrano-Andrés, L. *J. Phys. Chem. B* **2008**, *112*, 14096−14098.
(75) Kumar, S.; Sharma, N. D.; Davies, R. J. H.; Phillipson, D. W.; McCloskey, J. A. *Nucleic Acids Res.* **1987**, *15*, 1199−1216.
(76) Wei, H.; Cai, Q.; Rahn, R.; Zhang, X. *Free Radical Biol. Med.* **1997**, *23*, 148−154.
(77) Doorley, G. W.; Wojdyla, M.; Watson, G. W.; Towrie, M.; Parker, A. W.; Kelly, J. M.; Quinn, S. J. *J. Phys. Chem. Lett.* **2013**, *4*, 2739−2744.
(78) Zhang, Y.; de La Harpe, K.; Beckstead, A. A.; Improta, R.; Kohler, B. *J. Am. Chem. Soc.* **2015**, *137*, 7059−7062.
(79) Lin, C. H.; Patel, D. J. *Nat. Struct. Biol.* **1996**, *3*, 1046−1050.
(80) Hays, F. A.; Teegarden, A.; Jones, Z. J. R.; Harms, M.; Raup, D.; Watson, J.; Cavaliere, E.; Ho, P. S. *Proc. Natl. Acad. Sci. U. S. A.* **2005**, *102*, 7157−7162.
(81) Flinders, J.; Dieckmann, T. *J. Mol. Biol.* **2001**, *308*, 665−679.
(82) Thiviyanathan, V.; Yang, Y.; Kaluarachchi, K.; Rijnbrand, R.; Gorenstein, D. G.; Lemon, S. M. *Proc. Natl. Acad. Sci. U. S. A.* **2004**, *101*, 12688−12693.
(83) Kielkopf, C. L.; Ding, S.; Kuhn, P.; Rees, D. C. *J. Mol. Biol.* **2000**, *296*, 787−801.
(84) Weill, G.; Calvin, M. *Biopolymers* **1963**, *1*, 401−417.
(85) Sutherland, B. M.; Sutherland, J. C. *Biophys. J.* **1969**, *9*, 292−302.
(86) Markovitsi, D.; Onidas, D.; Gustavsson, T.; Talbot, F.; Lazzarotto, E. *J. Am. Chem. Soc.* **2005**, *127*, 17130−17131.
(87) Vayá, I.; Gustavsson, T.; Douki, T.; Berlin, Y.; Markovitsi, D. *J. Am. Chem. Soc.* **2012**, *134*, 11366−11368.

DOI: 10.1021/jacs.5b05140
J. Am. Chem. Soc. 2015, 137, 11656−11665